Eurasian Journal of Physics and Functional Materials

Volume 9 | Number 2

Article 4

Pages: 97 - 103

6-30-2025

Highly Dense Ba0.9La0.1Ce0.7Zr0.1Y0.15Zn0.05O3�δ Electrolyte Material for Intermediate Temperature Solid Oxide Fuel Cells

Md. Mosfiqur Rahman
Faculty of Integrated Technologies, Universiti Brunei Darussalam, Gadong, BE1410, Brunei, mosfiqurju35@gmail.com

Abu Hanjala
Department of Physics, Mawlana Bhashani Science and Technology University, Santosh, Tangail - 1902, Bangladesh

Muhammed Ali
Fuel Cell Institute, Universiti Kebangsaan Malaysia, 43600 UKM Bangi, Selangor, Malaysia

Lukman Ahmed Omeiza
Faculty of Integrated Technologies, Universiti Brunei Darussalam, Gadong, BE1410, Brunei

Veena Raj
Faculty of Integrated Technologies, Universiti Brunei Darussalam, Gadong, BE1410, Brunei

See next page for additional authors

Recommended Citation

Rahman, Md. Mosfiqur; Hanjala, Abu; Ali, Muhammed; Omeiza, Lukman Ahmed; Raj, Veena; Balela, Mary Donnabelle L.; and Azad, Abul Kalam (2025) "Highly Dense Ba0.9La0.1Ce0.7Zr0.1Y0.15Zn0.05O3�δ Electrolyte Material for Intermediate Temperature Solid Oxide Fuel Cells," *Eurasian Journal of Physics and Functional Materials*: Vol. 9: No. 2, Article 4.
DOI: https://doi.org/10.69912/2616-8537.1245

Highly Dense Ba0.9La0.1Ce0.7Zr0.1Y0.15Zn0.05O3�δ Electrolyte Material for Intermediate Temperature Solid Oxide Fuel Cells

Authors

Md. Mosfiqur Rahman, Abu Hanjala, Muhammed Ali, Lukman Ahmed Omeiza, Veena Raj, Mary Donnabelle L. Balela, and Abul Kalam Azad

ORIGINAL STUDY

Highly Dense $Ba_{0.9}La_{0.1}Ce_{0.7}Zr_{0.1}Y_{0.15}Zn_{0.05}O_{3-\delta}$ Electrolyte Material for Intermediate Temperature Solid Oxide Fuel Cells

Md. M. Rahman [a,b,*], Abu Hanjala [c], Muhammed Ali [d], Lukman A. Omeiza [a], Veena Raj [a], Mary D.L. Balela [e], Abul K. Azad [a,**]

[a] Faculty of Integrated Technologies, Universiti Brunei Darussalam, Gadong, BE1410, Brunei
[b] Faculty of Science & Information Technology, Daffodil International University, Dhaka, 1341, Bangladesh
[c] Department of Physics, Mawlana Bhashani Science and Technology University, Santosh, Tangail 1902, Bangladesh
[d] Fuel Cell Institute, Universiti Kebangsaan Malaysia, UKM Bangi, 43600, Selangor, Malaysia
[e] Sustainable Electronic Materials Group, Department of Mining, Metallurgical, and Materials Engineering, College of Engineering, University of the Philippines Diliman, Quezon City, 1101, Philippines

Abstract

A new perovskite-type polycrystalline $Ba_{0.9}La_{0.1}Ce_{0.7}Zr_{0.1}Y_{0.15}Zn_{0.05}O_{3-\delta}$ (BLCZYZn) electrolyte material was prepared by the solid-state reaction method in pure phase. The material was studied to understand the impact of co-doping of La^{3+} at the A-site and Zn^{2+} at the B-site to use in the intermediate temperature solid oxide fuel cells (IT-SOFCs). X-ray diffraction study shows that the material crystallizes in the phase purity with cubic symmetry in Pm-3m space group. Rietveld refinement of the XRD data shows the cell parameter a = 4.445 with 98.35 % relative density. Scanning electron microscopy images confirm the highly dense material with distinct grain boundaries. Thermogravimetric analysis shows about 0.30 % weight loss from RT to 1000 °C. Electrochemical impedance spectroscopy in air shows the ionic conductivity of 2.83×10^{-4} Scm^{-1} at 700 °C with the activation energy of 0.62 eV. This material indicates great prospects in using as electrolyte for IT-SOFCs.

Keywords: IT-SOFC, Perovskite, Electrochemical performance, XRD, Electrolyte

1. Introduction

Solid oxide fuel cells (SOFCs) have gained attention all over the world as one of the cleanest energy conversion devices that converts chemical energy into electricity by adopting electrochemical processes. SOFCs are highly efficient and environmentally friendly with fuel flexibility [1—3]. The typical SOFC operates at high temperatures (800—1000 °C) with some disadvantages such as thermal stress, material degradation, costly manufacturing etc. But intermediate temperature solid oxide fuel cell (IT-SOFC) that operates at 400—700 °C has shown promising result to overcome those disadvantages [4]. Irshad et al. [5] studied $BaCe_{0.97}Sm_{0.03}O_{3-\delta}$ and $BaCe_{0.97}Gd_{0.03}O_{3-\delta}$ electrolytes. Both of the electrolytes were found very dense and useful for IT-SOFC. The $BaCe_{0.5}Zr_{0.3}Y_{0.1}Yb_{0.05}Zn_{0.05}O_{3-\delta}$ electrolyte show high density and proton conductivity which is suitable for IT-SOFC application [6]. The studied electrolyte was found to be very dense with 98 % relative density. Their reported ionic conductivity was 0.0122 Scm^{-1} at 700 °C. Hossain et al. [7] investigated the $BaCe_{0.7}Zr_{0.1}Y_{0.15}Zn_{0.05}O_{3-\delta}$ electrolyte for the use in IT-SOFC. They found 96.76 % relative density with 0.01 Scm^{-1} ionic conductivity at 700 °C. The $BaZr_{0.8}Y_{0.2}O_{3-\delta}$ electrolyte was studied by Li et al. [8]. They found 95.6 % density with 0.0069 Scm^{-1} ionic conductivity in wet air at 700 °C. Radenahmad et al. [4] studied

---

Received 9 May 2025; revised 19 May 2025; accepted 20 May 2025.

* Corresponding author at: Faculty of Integrated Technologies, Universiti Brunei Darussalam, Gadong, BE1410, Brunei.
** Corresponding author.
E-mail addresses: mosfiqurju35@gmail.com (Md.M. Rahman), abul.azad@ubd.edu.bn (A.K. Azad).

https://doi.org/10.69912/2616-8537.1245

$Ba_{0.5}Sr_{0.5}Ce_{0.5}Zr_{0.35}Y_{0.1}Sm_{0.05}O_{3-\delta}$ electrolyte for use in IT-SOFC. Their reported ionic conductivity was 0.001159 Scm^{-1} in dry argon at 700 °C with 91 % relative density. Lyagaeva et al. [9] studied the $BaCe_{0.5}Zr_{0.3}Y_{0.1}Yb_{0.1}O_{3-\delta}$ electrolyte for IT-SOFC and found it highly dense with 97 % relative density. The $LaMg_{0.67}Nb_{0.33}O_3$ electrolyte was investigated by Gao et al. [1] for both of the intermediate and high temperature-based SOFCs and found 0.0023 Scm^{-1} ionic conductivity at 550 °C. Leng et al. [10] studied the $BaCe_{0\cdot7}Zr_{0\cdot1}Y_{0.1}Yb_{0.1}O_{3\text{-}\delta}$ electrolyte for the IT-SOFCs. The investigated ionic conductivity of this material was 0.03 Scm^{-1} at 700 °C. The La^{3+} co-doped $Ce_{0.8}La_{0.1}Ca_{0.1}O_{2-\delta}$ electrolyte for IT-SOFCs demonstrated an improved ionic conductivity of 1.06×10^{-1} S cm^{-1} at 800 °C, with an activation energy of 1.02 eV [11].

The absence of La^{3+} at the A-site and Zn^{2+} at the B-site can result in a lower level of oxygen vacancy concentration, which negatively affects ionic conductivity. This makes it less suitable for applications like intermediate-temperature solid oxide fuel cells (IT-SOFCs). In this paper, $Ba_{0.9}La_{0.1}Ce_{0.7}Zr_{0.1}Y_{0.15}Zn_{0.05}O_{3-\delta}$ (BLCZYZn) electrolyte material has been studied to comprehend its structural phase, surface morphology, thermal behavior, and electrochemical performance. For that, the material was synthesized and characterized by the solid state reaction method, X-ray diffraction, scanning electron microscopy, thermogravimetric analysis, and electrochemical impedance spectroscopy. The main aim of this study is to comprehend the co-doping of lanthanum (La^{3+}) at the A-site and zinc (Zn^{2+}) at the B-site of the ABO_3 perovskite structure.

2. Methodology

The $Ba_{0.9}La_{0.1}Ce_{0.7}Zr_{0.1}Y_{0.15}Zn_{0.05}O_{3-\delta}$ electrolyte was synthesized using the solid-state reaction method. Stoichiometric amounts of $BaCO_3$, La_2O_3, CeO_2, ZrO_2, Y_2O_3, and ZnO were mixed and ground with an agate mortar and pestle in acetone for approximately 1 h. The resulting mixture was then calcined in air at 1000 °C for 8 h. After the calcination, the oxide powder was grinded and mixed with acetone for another 1 h. Pellets with a diameter of 13 mm were formed using a hydraulic press at 5 tons and sintered at 1300 °C for 12 h. The structural properties of the mixed oxides were evaluated at room temperature using a Shimadzu-7000 diffractometer (CuKα_1, wavelength $\lambda = 1.5406$ Å) with a step size of 0.02° per minute across a 5°–80° range. Data refinement was performed using the Rietveld method [12]. The surface morphology and elemental composition were analyzed using a 4th generation NeoScope JCM-7000 along with EDX. Thermal behavior of the materials was assessed with a QMS 403 Aëolos® Quadro quadrupole mass spectrometer over a temperature range of 30 °C–1200 °C, with heating and cooling rates of 10 °C per minute. Electrochemical impedance spectroscopy (EIS) was conducted at open cell voltage using the Admiral Squidstat Plus, with a signal amplitude of 10 mV across a frequency range of 200 kHz to 0.1 Hz. For impedance measurements, pellets of $Ba_{0.9}La_{0.1}Ce_{0.7}Zr_{0.1}Y_{0.15}Zn_{0.05}O_{3-\delta}$ were sintered, polished, and coated with platinum paste symmetrically ($Pt/Ba_{0.9}La_{0.1}Ce_{0.7}Zr_{0.1}Y_{0.15}Zn_{0.05}O_{3-\delta}/Pt$) using a Quorum Q150RS sputter coater. Platinum paste was applied to the central area on both sides of each pellet, serving as a current collector with a size of approximately 6 mm. The pellets measured about 4 mm in thickness and 13 mm in diameter. Impedance measurements were taken in air from 500 °C to 800 °C at 50 °C intervals, with a heating rate of 3 °C/min. The impedance data was analyzed by Z-View software in which the brick-layer model was applied to model the electrical response of the samples.

3. Results and discussion

3.1. XRD analysis

Fig. 1 shows the XRD pattern of BLCZYZn. The Rietveld refinement and 3D structure of BLCZYZn are shown in Fig. 2(a) and (b), respectively. FullProf and Checkcell software were used to index the sintered material. The indexed pattern is crystallized in cubic symmetry with Pm-3m space group. A summary of Rietveld refinement results is presented in Table 1. Rietveld refinement also confirms that the material has cubic symmetry with Pm-3m space group. The lattice parameters of this material presented in Table 1 closely match with typical perovskite materials $BaZrO_3$ (a = b = c = 4.193 Å) [4,13] and $BaCeO_3$ (a = b = c = 4.445 Å) [4,14]. Since Y^{3+} (0.90 Å) and Zn^{2+} (0.74 Å) have closer ionic radii, both elements can occupy the B-site in the perovskite structure, ensuring the retention of cubic symmetry. The theoretical and empirical densities of the material are 6.174 g/cm^3 and 6.072 g/cm^3, respectively, resulting in 98.35 % relative density. The value of the goodness-fit parameter ($\chi^2 = 1.43$) represents good agreement between the observed and calculated pattern of X-ray diffraction.

3.2. Scanning electron microscopy

To prevent the mixing of gaseous reactants, the electrolyte material in an SOFC must be dense and gas-tight. Resistance at grain boundaries hinders the total conductivity of SOFCs. As grain size increases, the number of these barriers is reduced, decreasing resistance and increasing overall ionic conductivity.

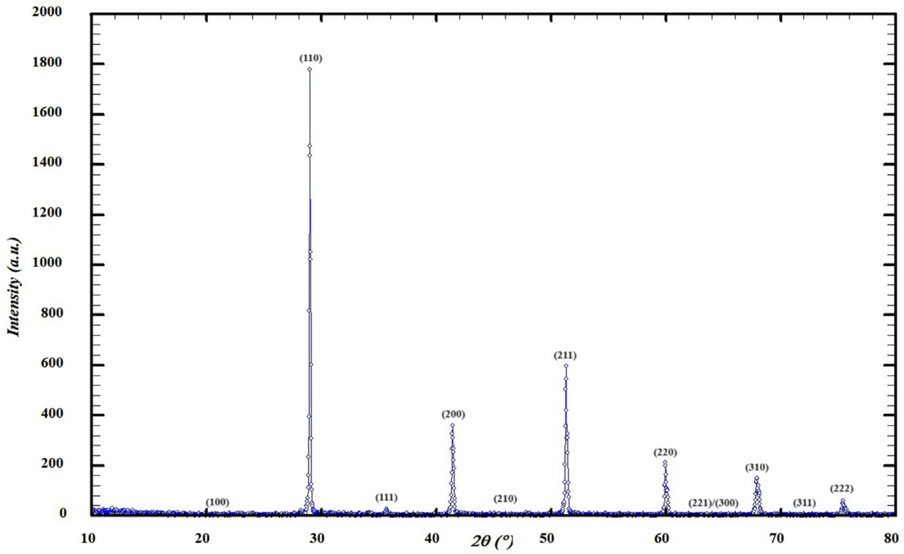

Fig. 1. XRD pattern of BLCZYZn.

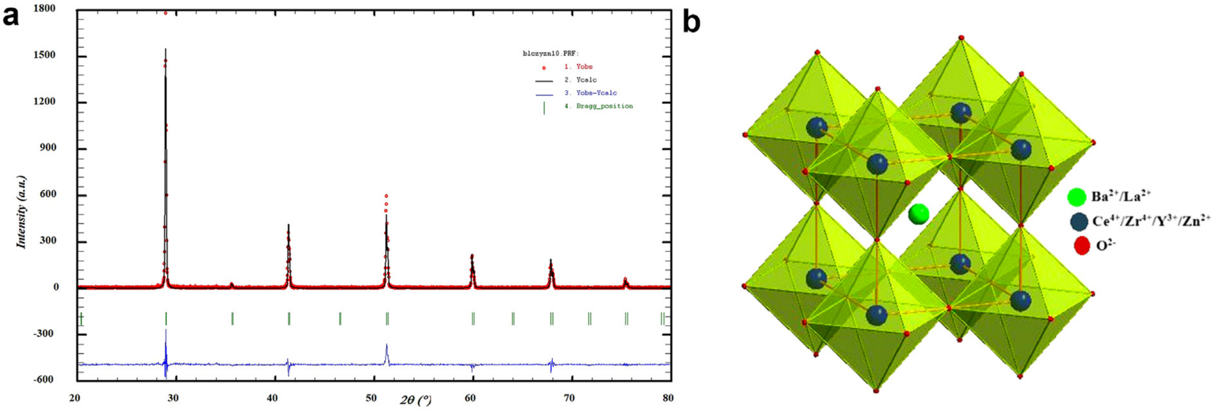

Fig. 2. ***(a)*** *Rietveld refinement profile of BLCZYZn.* ***(b)*** *3D Structure of BLCZYZn.*

Table 1. Rietveld refinement parameters of BLCZYZn.

Sample	Lattice parameter a = b = c (Å)	Unit cell volume (Å^3)	χ^2	R_f factor	R_p	R_{wp}	R_e	Theoretical density (g/cm^3)	Empirical density (g/cm^3)	Relative density (%)
BLCZYZn	4.3653	83.18	1.43	9.43	35.6	40.8	34.1	6.174	6.072	98.35

However, this adjustment may reduce the material's mechanical strength. The SEM images of BLCZYZn on pellet surface are shown in Fig. 3. The images were chosen with magnification (a) 10,000 X (b) 5000 X and (c) 2500 X. It has larger and smaller grain boundaries. Also, the material is found to be very dense, compact, crack and liquid free. The surface of the material is well connected and can pass the ions efficiently. Similar types of SEM images on electrolyte material were reported by Radenahmad et al. [4] and Hossain et al. [7] for use in IT-SOFCs. Hence, it can be used as an electrolyte material for IT-SOFCs. The elemental distribution (presented in Table 2) by EDX analysis nearly matches with estimated values based on the chemical formulas.

3.3. Thermal analysis

The thermal behavior of BLCZYZn is presented in Fig. 4. Thermal analysis was conducted in air, maintaining a temperature range of 30–1200 °C to comprehend the weight change and thermal

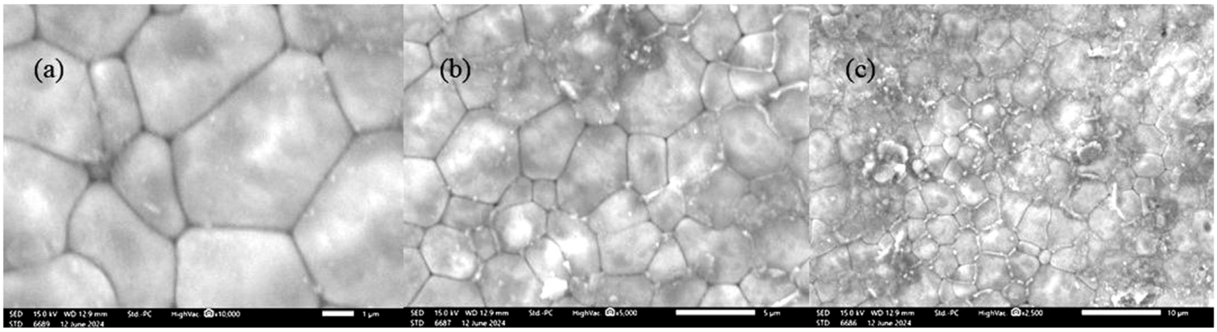

Fig. 3. SEM images of BLCZYZn.

Table 2. Elemental distribution of BLCZYZn.

Sample	BLCZYZn			
	Formula		EDX	
Element symbol	Weight (%)	Atomic (%)	Weight (%)	Atomic (%)
Ba	47.30	45	49.92	47.63
La	5.32	5	3.39	3.19
Ce	37.54	35	37.42	35
Zr	3.50	5	3.98	5.72
Y	5.10	7.50	4.07	6.01
Zn	1.25	2.5	1.22	2.45

degradation. The observed weight loss of BLCZYZn was approximately 0.30 % within the temperature range of 30—1000 °C. The initial weight loss of BLCZYZn below 400 °C was 0.03 %, attributed to the evaporation of absorbed water from the surroundings after final sintering. Additional weight loss begins around 400 °C, caused by the formation of oxygen vacancies and the valence adjustment of B-site cations. Since the weight loss of the material can affect the oxygen occupancy, the oxygen occupancy was calculated at 500—700 °C by using the formula, $3-\delta=3-\frac{weight\ of\ formula\times weight\ change}{atomic\ mass\ of\ O_2\times 100}$, where δ denotes the oxygen deficiency. Calculations show that BLCZYZn has an oxygen occupancy of 2.98 and a thermal change of 0.11 %. The observed weight stability is particularly notable due to the lower concentration of La (10 %) and higher concentration of Ba (90 %) at the A-site in the ABO_3 perovskite structure. This enhanced thermal stability makes the composition well-suited for use in IT-SOFCs.

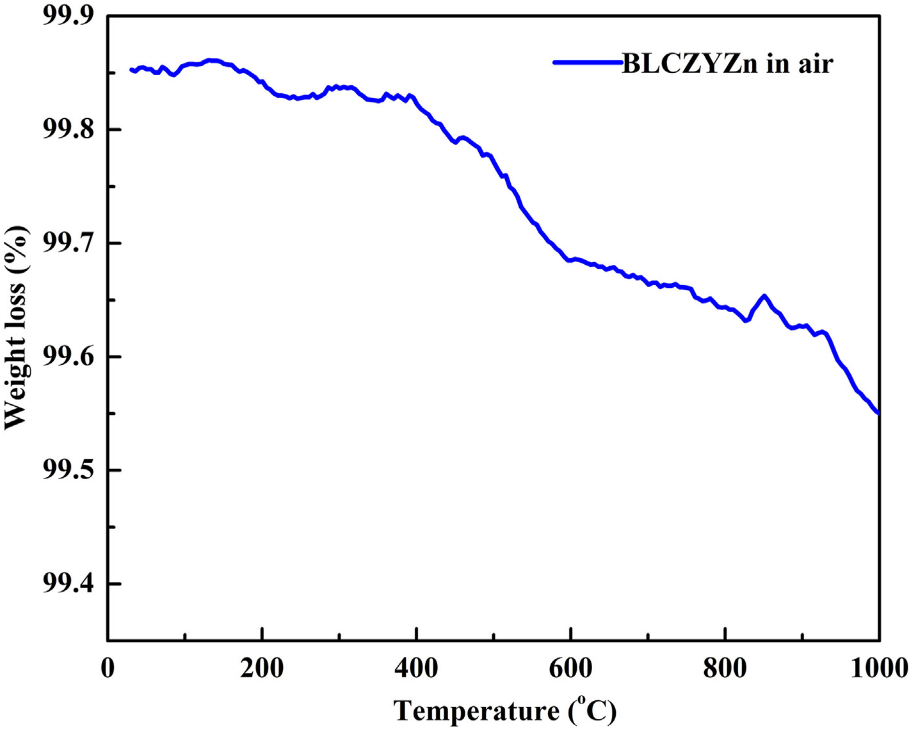

Fig. 4. TGA plot of BLCZYZn.

5. Electrochemical impedance spectroscopy

Electrochemical impedance spectroscopy was performed in air from 500 to 800 °C to assess the material's electrochemical performance. As impedance and conductivity are inversely proportional, low impedance suggests high ionic conductivity, which is key for proton transport in fuel cells. Therefore, material showing low impedance in this test is promising for fuel cell applications. For IT-SOFCs, the impedance spectra of BLCZYZn at 700 °C is presented in Fig. 5. Resistance was determined by fitting the impedance data to 3RC (resistance in combination with parallel to CPE) equivalent circuit model, and conductivity can be estimated using the following equation [4].

$$\sigma = 1/\rho = L/RA \tag{1}$$

where, σ, ρ,and R are denoted by conductivity, resistivity, and resistance, respectively. L and A, are denoted by the length and cross-sectional area, respectively.

Since conductivity is inversely proportional to resistivity, it can be maintained at higher temperatures according to the Arrhenius equation. The Arrhenius equation can be written [4] as,

$$\sigma = \sigma_0 e^{-E_a/RT} \tag{2}$$

where, σ, σ_0 and E_a are denoted by the conductivity, pre-exponential factor, and activation energy, respectively. R and T, are denoted by gas constant and temperature, respectively.

Fig. 6 represents the Arrhenius plot of total conductivity and activation energy of the BLCZYZn. The ionic conductivity of BLCZYZn is 2.83×10^{-4} Scm^{-1} in air at 700 °C and the activation energy of BLCZYZn is 0.62 eV, measured at 500—700 °C, as listed in Table 3. The conductivity exhibits a significant increase as the temperature rises within the range of 500 °C—800 °C. This phenomenon can be attributed to the effects of heat-driven atomic motion and ion transport. At elevated temperatures, the thermal energy supplied to the system enhances the mobility of atoms and ions. This increased mobility facilitates more efficient charge transport, thereby boosting the overall conductivity performance. The activation energy of this material is comparable to $\text{BaZr}_{0.8}\text{Y}_{0.2}\text{O}_{3-\delta}$ (0.61 eV) [15]. In proton-conducting perovskites, protons are expected to follow the Grotthuss mechanism [4,16,17], undergoing multiple transitions, especially at higher temperatures. The process involves: i) a proton attaching to an oxygen atom; ii) reorientation of the proton-oxygen bond due to surrounding oxygen atoms; and iii) proton transfer between neighboring oxygen atoms [18]. The binding energy between hydroxyl (OH*) and dopants varies by dopant type, with values of −0.26 eV for yttrium, −0.35 eV for ytterbium, and −0.58 eV for indium,

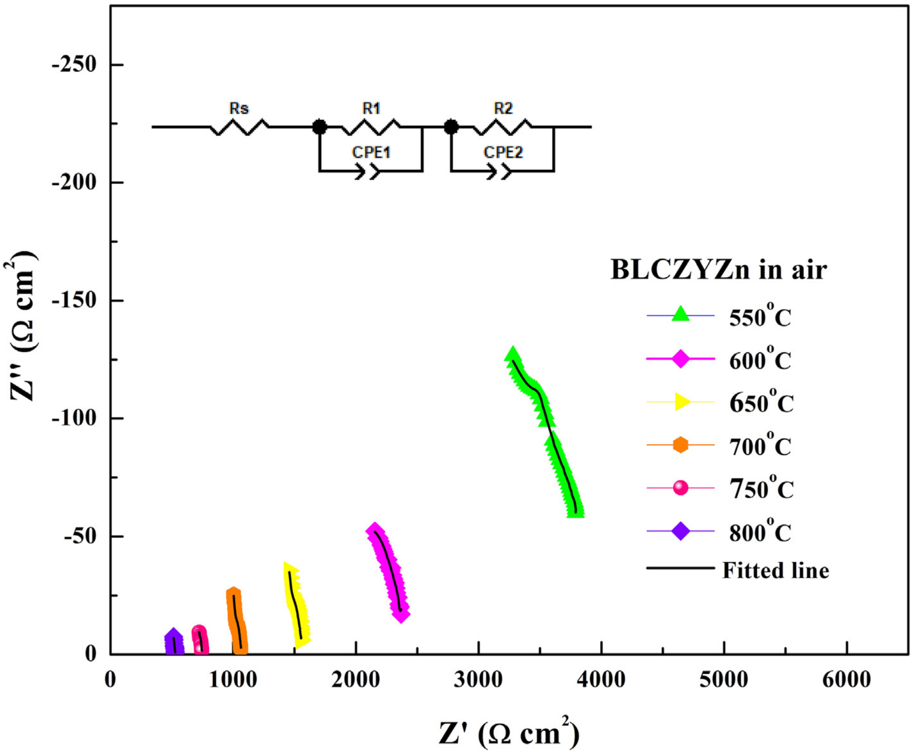

Fig. 5. Nyquist plot of BLCZYZn in air with inserted equivalent circuit.

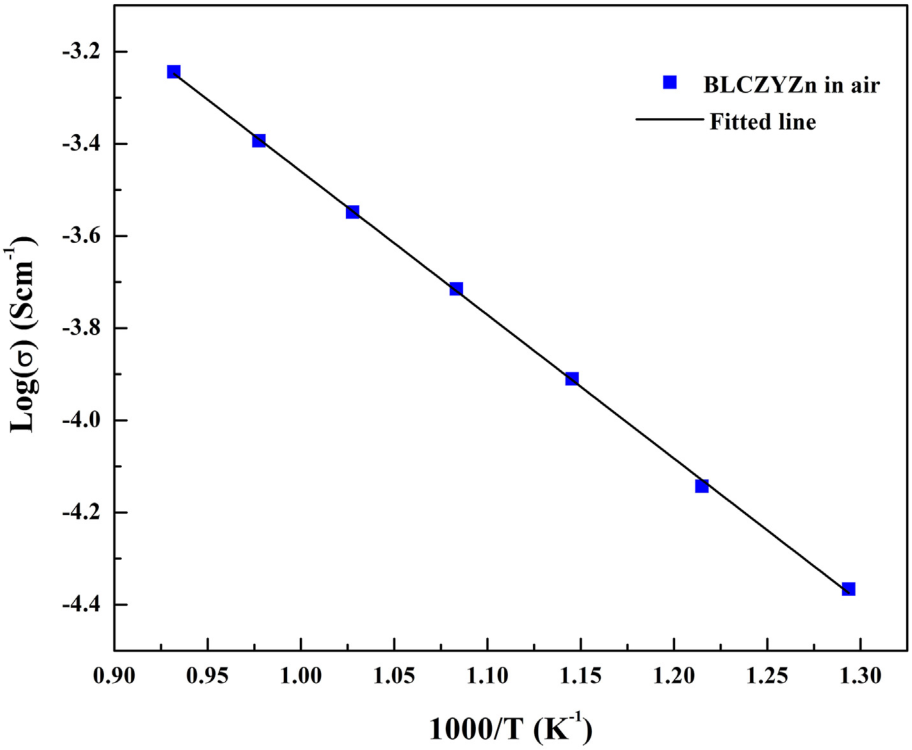

Fig. 6. Arrhenius plot of total conductivity of BLCZYZn.

Table 3. Conductivity and activation energy of BLCZYZn in air and some other related materials.

Sample	σ (Scm^{-1})		E_a (eV)	Reference
	500 °C	700 °C	500 °C–700 °C	
	Air	Air	Air	
BLCZYZn	4.30×10^{-5}	2.83×10^{-4}	0.62	This work
$BaCe_{0.7}Zr_{0.1}Y_{0.15}Zn_{0.05}O_{3-\delta}$		7.55×10^{-3} (dry H_2)		[7]
$BaCe_{0.5}Zr_{0.3}Y_{0.1}Yb_{0.05}Zn_{0.05}O_{3-\delta}$		1.22×10^{-2} (wet H_2)		[6]

aligning well with experimental data. More negative binding energies indicate stronger and more stable hydroxyl-dopant interactions [19].

6. Conclusion

The material BLCZYZn crystallizes with cubic symmetry in the Pm-3m space group, as confirmed by Rietveld refinement. SEM analysis reveals that the material is dense, compact, and exhibits a well-connected grain structure with both small and large grain boundaries. Additionally, the material shows minimal weight loss, approximately 0.30 %. Its activation energy of 0.62 eV suggests good ionic conductivity. However, further testing of BLCZYZn in H_2 atmospheres is planned to evaluate its potential as a proton-conducting electrolyte for use in IT-SOFCs.

Funding

The authors declare that no funds, grants, or other support were received for the manuscript.

Conflict of interest

The authors have no relevant financial or non-financial interests to disclose.

Acknowledgments

M.M.R and L.A.O acknowledge the support of Universiti Brunei Darussalam (UBD) graduate scholarship. M.M.R thankful to the Fuel Cell Institute, Universiti Kebangsaan Malaysia (UKM) for the lab support.

References

[1] J. Gao, et al., Development of high-performance perovskite La(Mg2/3Nb1/3)O3 electrolyte with hybrid protonic/oxide ion conduction for low-temperature solid oxide fuel cells, Int J Hydrogen Energy 50 (Jan. 2024) 361–373, https://doi.org/10.1016/j.ijhydene.2023.08.172.
[2] Md.M. Rahman, et al., Numerical modeling of ammonia-fueled protonic-ion conducting electrolyte-supported solid oxide fuel cell (H-SOFC): a brief review, Processes 11 (9) (Sep. 2023) 2728, https://doi.org/10.3390/pr11092728.

[3] S. Hossain, A.M. Abdalla, S.N.B. Jamain, J.H. Zaini, A.K. Azad, A review on proton conducting electrolytes for clean energy and intermediate temperature-solid oxide fuel cells, Renew Sustain Energy Rev 79 (May) (2017) 750—764, https://doi.org/10.1016/j.rser.2017.05.147.

[4] N. Radenahmad, A. Afif, M.I. Petra, S.M.H. Rahman, S. Eriksson, A.K. Azad, High conductivity and high density proton conducting Ba1−xSrxCe0.5Zr0.35Y0.1Sm0.05O3−δ (x = 0.5, 0.7, 0.9, 1.0) perovskites for IT-SOFC, Int J Hydrogen Energy 41 (27) (Jul. 2016) 11832—11841, https://doi.org/10.1016/j.ijhydene.2016.02.073.

[5] M. Irshad, et al., Synergistic role of Biomolecules and Biochelating agents in the sustainable development of an efficient BaCe0.97M0.03O3-δ (M = Sm, Gd) perovskite electrolyte for IT-SOFC, Ceram Int 49 (23) (Dec. 2023) 38360—38366, https://doi.org/10.1016/j.ceramint.2023.09.170.

[6] A. Afif, et al., Ceramic fuel cells using novel proton-conducting BaCe0.5Zr0.3Y0.1Yb0.05Zn0.05O3-δ electrolyte, J Solid State Electrochem 26 (1) (Jan. 2022) 111—120, https://doi.org/10.1007/s10008-021-05062-1.

[7] S. Hossain, et al., Highly dense and chemically stable proton conducting electrolyte sintered at 1200 °C, Int J Hydrogen Energy 43 (2) (Jan. 2018) 894—907, https://doi.org/10.1016/j.ijhydene.2017.11.111.

[8] Y. Li, et al., Improvement of sinterability of BaZr0.8Y0.2O3-δ for H2 separation using Li2O/ZnO dual-sintering aid, Ceram Int 44 (13) (Sep. 2018) 15935—15943, https://doi.org/10.1016/j.ceramint.2018.06.014.

[9] J. Lyagaeva, G. Vdovin, L. Hakimova, D. Medvedev, A. Demin, P. Tsiakaras, BaCe0.5Zr0.3Y0.2−xYbxO3−δ proton-conducting electrolytes for intermediate-temperature solid oxide fuel cells, Electrochim Acta 251 (Oct. 2017) 554—561, https://doi.org/10.1016/j.electacta.2017.08.149.

[10] Z. Leng, et al., The effect of sintering aids on BaCe0·7Zr0·1Y0.1Yb0.1O3-δ as the electrolyte of proton-conducting solid oxide electrolysis cells, Int J Hydrogen Energy 47 (79) (Sep. 2022) 33861—33871, https://doi.org/10.1016/j.ijhydene.2022.07.237.

[11] J. Manjanna, M.H. Jakati, N. Momin, Improved ionic conductivity of Ca-doped and Ca-La co-doped ceria electrolytes for intermediate temperature solid oxide fuel cells, J Alloys Compd 1005 (Nov. 2024) 176085, https://doi.org/10.1016/j.jallcom.2024.176085.

[12] S. Liu, X. Tan, K. Li, R. Hughes, Synthesis of strontium cerates-based perovskite ceramics via water-soluble complex precursor routes, Ceram Int 28 (3) (Jan. 2002) 327—335, https://doi.org/10.1016/S0272-8842(01)00098-0.

[13] R.L. Moreira, A. Dias, Comment on ‘Prediction of lattice constant in cubic perovskites’, J Phys Chem Solid 68 (8) (Aug. 2007) 1617—1622, https://doi.org/10.1016/j.jpcs.2007.03.050.

[14] J. Wu, R.A. Davies, M.S. Islam, S.M. Haile, Atomistic study of doped $BaCeO_3$: dopant site-selectivity and cation non-stoichiometry, Chem Mater 17 (4) (Feb. 2005) 846—851, https://doi.org/10.1021/cm048763z.

[15] E. Fabbri, A. Depifanio, E. Dibartolomeo, S. Licoccia, E. Traversa, Tailoring the chemical stability of Ba(Ce0.8−xZrx)Y0.2O3−δ protonic conductors for intermediate temperature solid oxide fuel cells (IT-SOFCs), Solid State Ion 179 (15—16) (Jun. 2008) 558—564, https://doi.org/10.1016/j.ssi.2008.04.002.

[16] N. Agmon, The Grotthuss mechanism, Chem Phys Lett 244 (5—6) (Oct. 1995) 456—462, https://doi.org/10.1016/0009-2614(95)00905-J.

[17] D. Marx, Proton Transfer 200 Years after von Grotthuss: Insights from Ab Initio Simulations, ChemPhysChem 7 (9) (Sep. 2006) 1848—1870, https://doi.org/10.1002/cphc.200600128.

[18] Z. Shi, W. Sun, W. Liu, Synthesis and characterization of BaZr0.3Ce0.5Y0.2−xYbxO3−δ proton conductor for solid oxide fuel cells, J Power Sources 245 (Jan. 2014) 953—957, https://doi.org/10.1016/j.jpowsour.2013.07.060.

[19] M.S. Islam, P.R. Slater, J.R. Tolchard, T. Dinges, Doping and defect association in AZrO3(A = Ca, Ba) and LaMO3(M = Sc, Ga) perovskite-type ionic conductors, Dalton Trans (2003) 19 (2004) 3061, https://doi.org/10.1039/b402669c.